Smoothing of time-optimal feedrates for Cartesian CNC machines

Casey L. Boyadjieff, Rida T. Farouki, and Sebastian D. Timar
clboyadjieff@ucdavis.edu, farouki@ucdavis.edu, sdtimar@ucdavis.edu

Department of Mechanical and Aeronautical Engineering,
University of California, Davis, CA 95616, USA.

Abstract. Minimum–time traversal of curved paths by Cartesian CNC machines, subject to prescribed bounds on the magnitude of acceleration along each axis, usually involves a "bang–bang" control strategy in which the acceleration bound is realized by one or another of the machine axes at each instant during the motion. For a path specified by a polynomial parametric curve and prescribed acceleration bounds, the time–optimal feedrate may be expressed in terms of a C^0 piecewise–rational function of the curve parameter. This function entails sudden changes in either the identity of the limiting axis, or the sign of acceleration on a single limiting axis, incurring demands for instantaneous changes of motor torque that may not be physically realizable. A scheme is proposed herein to generate smoothed C^1 (slightly sub–optimal) feedrate functions, that incur only finite rates of change of motor torque and remain consistent with the axis acceleration bounds. An implementation on a 3–axis CNC mill driven by an open–architecture software controller is used to illustrate this scheme.

1 Introduction

When a system of bounded motive force is commanded to execute a given spatial path, it is natural to ask: what control strategy, consistent with the motive–force constraints, yields the minimum traversal time? Suppose the path is a straight line, to be traversed by a rocket capable of equal maximum forward and reverse thrust, that starts and ends at rest and is free of external forces. The obvious answer in this case is to accelerate with maximum forward thrust to the midpoint and then to apply maximum reverse thrust for the second half of the traversal. This type of solution is known as "bang-bang" control, since it involves operation at the limits of the motive–force constraints throughout the entire motion, and is characteristic of most time-optimal control schemes [9, 12].

Time–optimal feedrates are of interest in *high–speed machining* [11, 16, 19] where the traversal of strongly–curved paths at high feedrates can cause inertial effects to dominate cutting forces, friction, etc. However, time–optimal feedrates for Cartesian CNC machines subject to prescribed axis acceleration bounds are in general continuous, but non–differentiable at certain *switching points* or *break points* along the curved path. The resulting discontinuities in feed acceleration (rate of change of feedrate) along the curved path imply instantaneous changes

in the output torque of the motors that drive the machine axes, which are not physically realizable. The goal of this study is to develop a simple automatic means of smoothing time–optimal feedrates so as to remove the feed acceleration discontinuities, without significantly increasing the overall path traversal time or violating the original axis acceleration constraints.

This paper is organized as follows. Section 2 provides a brief summary of the time–optimal feedrate problem for acceleration–limited Cartesian CNC machines executing paths specified by polynomial parametric curves [18]. The procedure for smoothing the C^0 break points and switching points of these feedrates is then developed in Section 3, together with a method for ensuring that the smoothed feedrate does not violate the original acceleration constraints. In Section 4 we describe the real–time CNC interpolator algorithm for the smoothed feedrate. Finally, Section 5 provides experimental validation of the smoothing process through implementation on a 3–axis open–architecture CNC mill, and Section 6 summarizes our present results and makes some concluding remarks.

2 Time–optimal feedrates

The time–optimal feedrate problem was first studied in the context of robotics [2, 13–15] — typically for systems with revolute joints. In a previous study [18] we have applied these methods to Cartesian CNC machines. The latter context is attractive, because it admits computation of a closed–form expression for the time–optimal feedrate when the path is specified as a polynomial parametric curve. The differential equation that governs the extremal acceleration phases can be solved analytically, and the break points and switching points delineating such phases can be computed using only a univariate polynomial root solver.

Since it is rather involved, we refer the reader to [18] for complete details[1] of the time–optimal feedrate algorithm. Our focus in this paper is on developing a post–processing step, employed to smooth thetangent–discontinuous points that arise generically in the time–optimal feedrate. The smoothed feedrate, although slightly sub–optimal, is less taxing on the axis drive motors since it does not demand instantaneous changes in the axis motor output torque.

2.1 Path geometry and kinematics

Consider a path specified [4] by a degree–n Bézier curve

$$\mathbf{r}(\xi) \;=\; \sum_{k=0}^{n} \mathbf{p}_k \binom{n}{k} (1-\xi)^{n-k} \xi^k \,, \qquad \xi \in [\,0,1\,]$$

with control points $\mathbf{p}_k = (x_k, y_k, z_k)$ for $k = 0, \ldots, n$. If s denotes cumulative arc length along the curve, the *parametric speed* $\sigma(\xi)$ of this curve is defined by

$$\sigma(\xi) \;=\; \frac{\mathrm{d}s}{\mathrm{d}\xi} \;=\; |\mathbf{r}'(\xi)|$$

[1] See also [17] for an extension of the algorithm to accommodate finite axis velocity bounds as well as acceleration bounds.

and the unit tangent and normal vectors and curvature are defined by

$$\mathbf{t} = \frac{\mathbf{r}'}{\sigma}, \qquad \mathbf{n} = \frac{\mathbf{r}' \times \mathbf{r}''}{|\mathbf{r}' \times \mathbf{r}''|} \times \mathbf{t}, \qquad \kappa = \frac{|\mathbf{r}' \times \mathbf{r}''|}{\sigma^3}. \tag{1}$$

The feedrate v is the derivative $\mathrm{d}s/\mathrm{d}t$ of arc length with respect to time, while $a = \mathrm{d}v/\mathrm{d}t$ is called the *feed acceleration*. Derivatives with respect to time t and the curve parameter ξ, denoted by dots and primes respectively, are related by

$$\frac{\mathrm{d}}{\mathrm{d}t} = \frac{\mathrm{d}s}{\mathrm{d}t}\frac{\mathrm{d}\xi}{\mathrm{d}s}\frac{\mathrm{d}}{\mathrm{d}\xi} = \frac{v}{\sigma}\frac{\mathrm{d}}{\mathrm{d}\xi}. \tag{2}$$

In terms of v and a, the velocity and acceleration vectors along the curve may be written as

$$\mathbf{v} = \dot{\mathbf{r}} = v\,\mathbf{t}, \qquad \mathbf{a} = \ddot{\mathbf{r}} = a\,\mathbf{t} + \kappa v^2\,\mathbf{n}.$$

Given a suitable feedrate function $v(\xi)$ for the path $\mathbf{r}(\xi)$, the real–time CNC interpolator algorithm within the machine control software computes a *reference point* within each sample interval of the digital controller. The difference between the reference point and the actual machine position, as measured by encoders on the machine axes, constitutes the error signal for the control loop.

2.2 Construction of the time–optimal feedrate

Using relations (1) and (2) and noting that $\mathbf{r}' \cdot \mathbf{r}'' = \sigma\sigma'$ allows the acceleration vector to be written as

$$\mathbf{a} = \frac{vv'}{\sigma^2}\,\mathbf{r}' + \frac{v^2}{\sigma^3}\,(\sigma\mathbf{r}'' - \sigma'\mathbf{r}').$$

It is convenient to work with the *square* of the feedrate, which we denote by $q = v^2$. In terms of q and its derivative $q' = 2vv'$ the components of the acceleration along each axis may be expressed as

$$\begin{aligned} a_x &= \frac{q'}{2\sigma^2}\,x' + \frac{q}{\sigma^3}\,(\sigma x'' - \sigma' x'), \\ a_y &= \frac{q'}{2\sigma^2}\,y' + \frac{q}{\sigma^3}\,(\sigma y'' - \sigma' y'), \\ a_z &= \frac{q'}{2\sigma^2}\,z' + \frac{q}{\sigma^3}\,(\sigma z'' - \sigma' z'). \end{aligned} \tag{3}$$

For a given path $\mathbf{r}(\xi)$, the time–optimal feedrate problem consists of determining the function $v(\xi)$ that will minimize the integral

$$T = \int_0^1 \frac{\sigma(\xi)}{v(\xi)}\,\mathrm{d}\xi$$

subject for all $\xi \in [0,1]$ to the constraints

$$-A_x \le a_x \le +A_x, \quad -A_y \le a_y \le +A_y, \quad -A_z \le a_x \le +A_z, \tag{4}$$

where A_x, A_y, A_z are prescribed acceleration bounds for the machine axes.

Complete details on the solution of this problem were presented in [18]. We content ourselves here with summarizing some key points that are pertinent to the feedrate smoothing problem. Observing that $q' = 2\sigma a$, the three inequalities (4) are linear in q and a, and each defines a strip of feasible states in the (q, a) plane. The intersection of these three strips yields a six–sided parallelogram of feasible (v^2, a) combinations, and of course only the portion in the right half of the plane ($v^2 > 0$) is physically meaningful (see Figure 1).

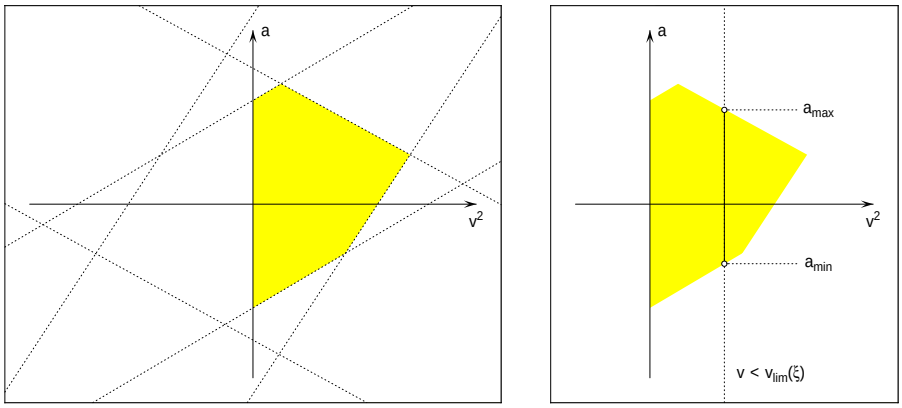

Fig. 1. Left: The constraints (4) define the set of feasible states as the portion of a six–sided parallelogram in the right half of the (v^2, a) plane. Right: any feedrate lower than the velocity limit $v_{\lim}(\xi)$ yields a range $a_{\min} \le a \le a_{\max}$ of feasible feed accelerations.

At each point of the path $\mathbf{r}(\xi)$, the right–most vertex of the parallelogram shown in Figure 1 defines the maximum possible feedrate $v_{\lim}(\xi)$ consistent with the constraints (4). The graph of $v_{\lim}(\xi)$ in the (ξ, v) plane is the *velocity limit curve* (VLC). This graph is continuous, but not differentiable everywhere — it exhibits slope discontinuities at *critical points*, where there is a change in the identity of the constraints defining the right–most parallelogram vertex.

The construction of the time–optimal feedrate function is performed in the (ξ, q) plane, below the "forbidden region" bounded by the VLC. At points below the VLC, there is a range $[\, a_{\min}, a_{\max} \,]$ of feasible feed accelerations, and in general the optimal feedrate $q(\xi)$ is a piecewise–analytic function whose segments correspond alternately to integrating the differential equations $a = a_{\max}(\xi, v)$ and $a = a_{\min}(\xi, v)$. Transitions between consecutive $a_{\max}$ and $a_{\min}$ phases are called *switching points*, since they signal a change in the identity of the limiting acceleration constraint. In general, some switching points lie on the VLC and others are situated below it. Besides switching points, the time–optimal feedrate generically exhibits other types of break points, corresponding to turning points, inflections, equi–orientation points, and transition points — see [18] for further details and a complete algorithm description.

Consider the form of the time–optimal feedrate function during an extremal acceleration phase. If x is the limiting axis, taking (4) with equality yields

$$\frac{q'}{2\sigma^2}\,x' \;+\; \frac{q}{\sigma^3}\,(\sigma x'' - \sigma' x') \;=\; \alpha_x A_x$$

or

$$q' \;+\; 2\left(\frac{x''}{x'} - \frac{\sigma'}{\sigma}\right) q \;=\; \alpha_x\,\frac{2A_x\sigma^2}{x'}\,, \tag{5}$$

where the quantity $\alpha_x = \pm 1$ identifies $a_{\max}/a_{\min}$ phases. The linear differential equation (5) admits the closed–form solution

$$q \;=\; \left(\frac{\sigma}{x'}\right)^2 (C + 2\alpha_x A_x x)\,, \tag{6}$$

with the integration constant C determined from a known point (ξ_*, q_*) of the trajectory. Similar expressions hold if y or z, rather than x, is the limiting axis.

2.3 Illustrative example

Figure 2 shows a typical example of the time–optimal feedrate computation for a planar Bézier curve with axis acceleration bounds $A_x = A_y = 10^4$ in/min^2. The time–optimal feedrate $q(\xi)$ can be represented exactly as a piecewise–rational function with five switching points: one is a critical point on the VLC, one is a tangency of an $a_{\min}/a_{\max}$ trajectory with the VLC, and the remaining three are intersections of $a_{\min}$ and $a_{\max}$ trajectories below the VLC.

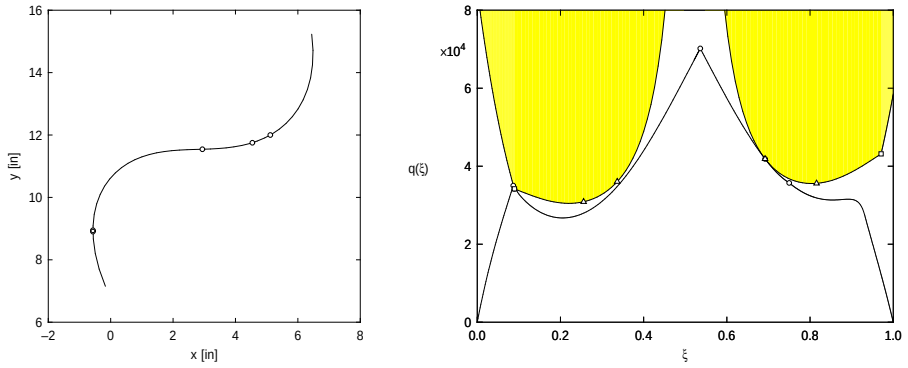

Fig. 2. Test curve (left) and construction of time–optimal feedrate along it (right). The region of infeasible states above the VLC is shown shaded. The time–optimal squared feedrate $q(\xi)$ is a piecewise–rational function with three switching points below the VLC (circles) and two switching points on the VLC (squares denote VLC critical points, and triangles denote tangency points of $a_{\max}$ or $a_{\min}$ trajectories with the VLC).

3 Smoothing of time–optimal feedrates

To maintain a near–time–optimal form for the smoothed feedrate, we adopt a strategy that inserts a short smoothing segment centered on each C^0 break point or switching point of the exact time–optimal feedrate. With this approach, most of the time–optimal feedrate is left unmodified, and the smoothing segments are designed to meet the unaltered segments with C^1 or C^2 continuity.

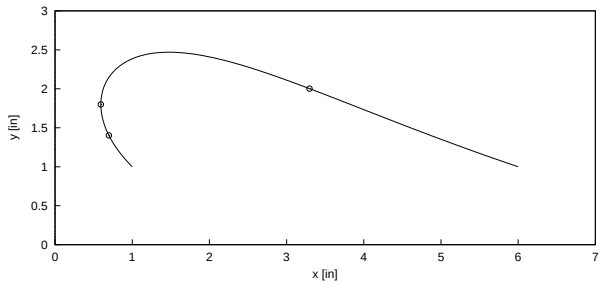

Fig. 3. Quintic Bézier curve with two switching points and an intermediate break point indicated, delineating the three segments of the time–optimal feedrate function.

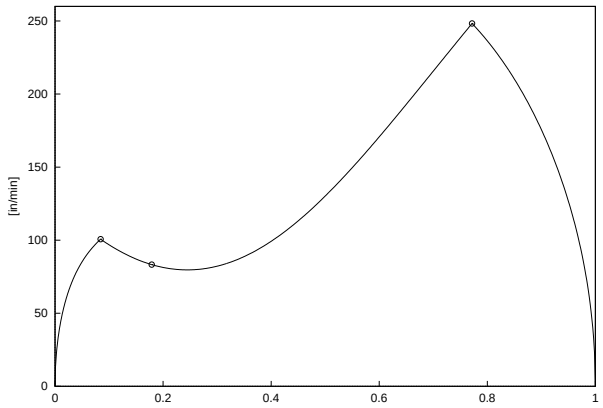

Fig. 4. Time–optimal feedrate v versus curve parameter ξ for the Bézier curve shown in Figure 3, with switching points between feedrate segments denoted by circles.

To illustrate the need for feedrate smoothing, we show in Figure 4 the time–optimal feedrate for the Bézier curve in Figure 3. This feedrate exhibits two switching points that incur feed acceleration discontinuities, and an intermediate

break point defined by a path turning point. Figure 5 indicates the individual x and y axis accelerations resulting from application of the time–optimal feedrate to the specified path. The bang–bang nature of the motion is clearly apparent, with either the x or y axis exhibiting saturation at the prescribed acceleration limits $\pm 10,000\,\mathrm{in/min}^2$ throughout the entire traversal (for simplicity we employ planar tool paths as examples: the extension to spatial paths is straightforward).

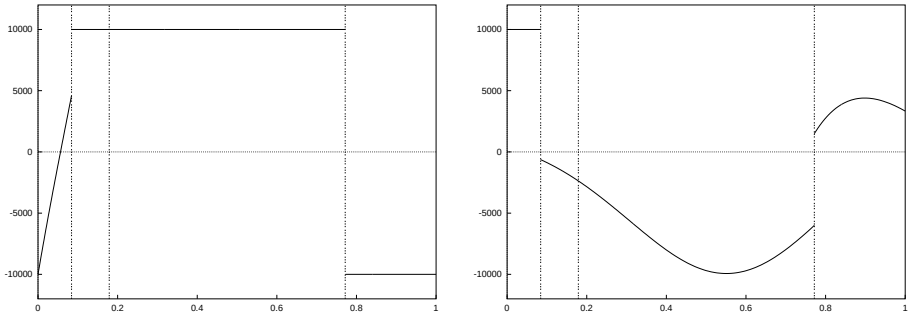

Fig. 5. Accelerations of the x axis (left) and y axis (right) in $\mathrm{in/min}^2$ versus the curve parameter ξ for time–optimal traversal of the curve shown in Figure 3. On the first curve segment, the acceleration is saturated at the upper bound on the y axis, while on the second and third segments it is saturated at the upper and lower bounds on the x axis. Note the acceleration discontinuities in both the x and y axes at the switching points, which demand instantaneous changes in output torque of the axis drive motors.

3.1 Form of feedrate–smoothing segments

The first step in the smoothing process is to identify all C^0 break points and switching points ξ_k in the exact time–optimal feedrate, and to define a smoothing interval $[\,\xi_l, \xi_r\,]$ of width $\Delta\xi_k = \xi_r - \xi_l$ centered on each. On this interval, the function $q(\xi)$ giving the square of the exact feedrate is replaced by the form

$$q_s(\xi) \;=\; \frac{\sigma^2(\xi)}{w^2(\xi)} \qquad \text{for } \xi \in [\,\xi_l, \xi_r\,]\,. \tag{7}$$

Here the parametric speed $\sigma(\xi)$ is determined by the curve $\mathbf{r}(\xi)$, while $w(\xi)$ is a polynomial whose coefficients will be used to match the endpoint values and derivatives of the smoothing feedrate segment with the unmodified time–optimal segments at the interval end–points ξ_l, ξ_r. Each C^0 point ξ_k of the time–optimal feedrate has an individually–determined polynomial $w(\xi)$.

Specifying the smoothing function $w(\xi)$ as a quintic allows the modified feed segment to match the unmodified feedrate segments with C^2 continuity (or C^1 continuity with two residual degrees of freedom available for shape adjustment).

This polynomial is defined in Bernstein form using a normalized parameter by

$$w(u) \;=\; \sum_{k=0}^{5} w_k \binom{5}{k} (1-u)^{5-k} u^k \,, \qquad \text{where } u \;=\; \frac{\xi - \xi_l}{\xi_r - \xi_l} \,.$$

The coefficients w_0, w_1 and w_4, w_5 allow for interpolation of end–point values and first derivatives of the time–optimal feed segments, while w_2 and w_3 yield the additional degrees of freedom. These degrees of freedom may be used to ensure that the modified feedrate segment will be traversed in an integer number of time steps of the digital controller.

The specific form (7) of the smoothing element is motivated by the desire to have a closed–form reduction of the integral arising in the real–time interpolator algorithm (described in Section 4 below). In terms of the normalized parameter u, the elapsed time along this segment with the feedrate (7) is

$$t(u) \;=\; \int_0^u \frac{\sigma}{v}\, \mathrm{d}u \;=\; \int_0^u w \; \mathrm{d}u$$

and hence $t(u)$ is simply a polynomial, since w is a polynomial in u.

3.2 Matching end–point values and derivatives

For each switching point ξ_k with smoothing interval $[\,\xi_l, \xi_r\,]$ a unique quintic smoothing function may be obtained by matching the values and first and second derivatives of the smoothing segment to those of the time–optimal feedrate at the interval endpoints ξ_l, ξ_r. The first and second derivatives of the smoothing segment (7) with respect to ξ are

$$\begin{aligned} q' &= \frac{2\sigma(\sigma' w - \sigma w')}{w^3} \,, \\ q'' &= \frac{2(\sigma\sigma'' + \sigma'^2)}{w^2} \;-\; \frac{2(\sigma^2 w'' + 4\sigma\sigma' w')}{w^3} \;+\; \frac{6\sigma^2 w'^2}{w^4} \,. \end{aligned} \tag{8}$$

Re–arranging (7) and (8) to write w, w', w'' on the left then gives

$$\begin{aligned} w &= \frac{\sigma}{\sqrt{q}} \,, \\ w' &= \frac{2\sigma\sigma' w - q' w^3}{2\sigma^2} \,, \\ w'' &= \frac{3w'^2}{w} \;-\; \frac{4\sigma' w'}{\sigma} \;+\; \frac{2w(\sigma\sigma'' + \sigma'^2) - q'' w^3}{2\sigma^2} \,. \end{aligned} \tag{9}$$

Taking first and second derivatives of $w(u)$ and relating $u \in [\,0,1\,]$ to $\xi \in [\,\xi_l, \xi_r\,]$ then yields the following expressions for the coefficients of $w(u)$:

$$\begin{aligned} &w_0 = w(\xi_l)\,, \quad w_1 = w_0 + \frac{\Delta\xi_k\, w'(\xi_l)}{5} \,, \quad w_2 = 2w_1 - w_0 + \frac{(\Delta\xi_k)^2\, w''(\xi_l)}{20} \,, \\ &w_5 = w(\xi_r)\,, \quad w_4 = w_5 - \frac{\Delta\xi_k\, w'(\xi_r)}{5} \,, \quad w_3 = 2w_4 - w_5 + \frac{(\Delta\xi_k)^2\, w''(\xi_r)}{20} \,. \end{aligned}$$

The factors of $\Delta\xi_k$ and $(\Delta\xi_k)^2$ arise from the fact that

$$\frac{\mathrm{d}w}{\mathrm{d}\xi} = \frac{1}{\Delta\xi_k}\frac{\mathrm{d}w}{\mathrm{d}u}\,.$$

3.3 Adjustment for integer number of time steps

Because CNC machine controllers employ digital time sampling, it is desirable to adjust the smoothing function slightly to ensure that the smoothing segment may be traversed in an integer number of time steps Δt. This can be accomplished while maintaining C^1 continuity between the smoothed and unmodified feedrate segments by adjusting only the middle two coefficients w_2, w_3 of the smoothing function. The total traversal time T for the smoothed feedrate segment is

$$T = \Delta\xi_k \int_0^1 w \,\mathrm{d}u = \frac{\Delta\xi_k}{6}\sum_{k=0}^{5} w_k\,. \tag{10}$$

The total time is divided by the sampling interval Δt to give the nominal number of steps needed for the smoothing segment. This number is then rounded up to the nearest integer value N, and a new traversal time T_{new} corresponding to an integer number of time steps is defined by $T_{\mathrm{new}} = N\Delta t$.

Multiplying the middle two control points of (10) by a scaling factor k and equating with T_{new} gives

$$T_{\mathrm{new}} = \frac{\Delta\xi_k}{6}\left[\, w_0 + w_1 + k(w_2 + w_3) + w_4 + w_5 \,\right],$$

and hence the appropriate value of the scaling factor is

$$k = \frac{6\,T_{\mathrm{new}}/\Delta\xi_k - (w_0 + w_1 + w_4 + w_5)}{w_2 + w_3}\,. \tag{11}$$

Once the coefficients w_2 and w_3 have been multiplied by k, the resulting time function will correspond to an integer number of time steps for traversal of the smoothed feedrate segment.

3.4 Compatibility with acceleration constraints

Using a smoothed feedrate segment of the form (7) with end–point values and derivatives matched to those of the unmodified time–optimal feedrate does not automatically guarantee that the smoothed segment will be compatible with the axis acceleration constraints (4). Requiring the smoothed feedrate to be less than or equal to the original time–optimal feedrate does not *per se* ensure the satisfaction of these constraints. Thus, an additional step is required to check that the smoothed feedrate does not violate these constraints.

For the smoothing feedrate segment (7) the axis accelerations (3) are

$$a_x = \frac{wx'' - w'x'}{w^3}\,, \qquad a_y = \frac{wy'' - w'y'}{w^3}\,. \tag{12}$$

Applying the smoothing algorithm described above to a variety of time–optimal feedrates and evaluating (12) indicates that in most cases the modified feedrate segments do satisfy the acceleration constraints, but in some cases the size of the smoothing interval $\Delta\xi_k$ may require adjustment.

Starting with a nominal smoothing interval of $\Delta\xi_k = 0.08$, and incrementally reducing this interval if violations of the acceleration constraints occur, appears to be a satisfactory approach to satisfying the constraints in all cases. A lower bound on $\Delta\xi_k$ (and the corresponding number of time steps) is imposed by the need for an integer number of time steps. Rounding up for an integer number of time steps has little effect when the total number of time steps is large, but rounding a segment up from a low number of steps can cause an oscillatory smoothed feedrate, incurring acceleration constraint violations. To preserve a near–time–optimal form for the modified feedrate, an upper bound on $\Delta\xi_k$ must also be imposed so that the smoothing segments account for a relatively small fraction of the overall feedrate profile. Assuming equal, symmetric acceleration constraints ($A_x = A_y = A$, say) gives

$$-A \le \frac{wx'' - w'x'}{w^3} \le +A \qquad \text{and} \qquad -A \le \frac{wy'' - w'y'}{w^3} \le +A\,,$$

or

$$\begin{aligned} wx'' - w'x' - w^3A &\le 0\,, \qquad wy'' - w'y' - w^3A \le 0\,, \\ wx'' - w'x' + w^3A &\ge 0\,, \qquad wy'' - w'y' + w^3A \ge 0\,, \end{aligned} \tag{13}$$

for the axis acceleration bounds on a smoothed feedrate segment.

All four of the inequalities (13) must be satisfied to assure that there are no acceleration constraint violations. To verify this, the coefficients of each of the four polynomials on the left are examined. If all the coefficients are of the same sign, and are greater than or equal to zero or less than or equal to zero, as appropriate, the constraints are satisfied. However, coefficients of mixed sign do not necessarily signal a constraint violation over the smoothing interval. In the case mixed–sign coefficients, a Sturm sequence [8, 21] may be used to verify if the bounding function has any roots within the smoothing interval. If no roots are indicated, the bound is satisfied. Otherwise, a shorter smoothing interval must be used to avoid violation of an acceleration constraint.

3.5 Smoothing example

To illustrate the smoothing process, a step–by–step smoothing of the time–optimal feedrate shown in Figure 7, for the path in Figure 6, is described below. In this example, there are four switching points that require feedrate smoothing and an additional three break points (corresponding to path turning points) that do not require smoothing. For simplicity, a single smoothing interval $\Delta\xi = 0.06$ will be used, centered about each of the four switching points ξ_k. Each of these points is smoothed individually as follows.

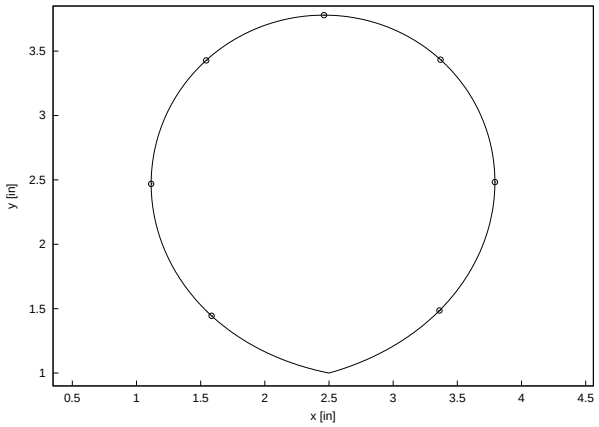

Fig. 6. Quintic Bézier curve with break points and switching points between feedrate segments indicated by circles. The curve starts and ends at the point $(x, y) = (2.5, 1.0)$.

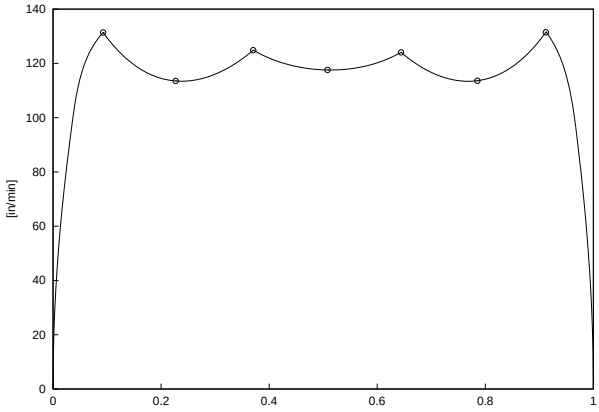

Fig. 7. The time–optimal feedrate v (for acceleration bounds $A = \pm 10,000$ in/min^2 on both axes) versus the parameter ξ along the curve in Figure 6, with break points and switching points indicated by circles.

1. Starting with the left–most switching point to be smoothed and referring to it as ξ_1, the left and right smoothing interval endpoints ξ_l and ξ_r are simply $\xi_l = \xi_1 - \frac{1}{2}\Delta\xi$ and $\xi_r = \xi_1 + \frac{1}{2}\Delta\xi$.
2. The squared time–optimal feedrate $q(\xi)$ along with its derivatives $q'(\xi)$, $q''(\xi)$ and the parametric speed $\sigma(\xi)$ and its derivatives $\sigma'(\xi)$, $\sigma''(\xi)$ are evaluated at ξ_l and ξ_r for use in (9) to determine values for $w(\xi)$, $w'(\xi)$, $w''(\xi)$ at ξ_l and ξ_r. With the desired values of w and its derivatives known at the smoothing interval endpoints, coefficients for the smoothing function $w(u)$, defined on $u \in [\,0, 1\,]$, are determined.
3. The function $w(u)$ is integrated over $[\,0, 1\,]$ to obtain the traversal time T for the smoothing segment, and a new traversal time T_{new} corresponding to an integer number of sampling intervals Δt is obtained from $T_{\text{new}} = \lceil T/\Delta t \rceil\ \Delta t$. The time factor k is given by (11) and once w_2 and w_3 have been multiplied by k, we are assured that the smoothed segment will be completed in a whole number of time steps of the digital controller.
4. The smoothed feedrate segment is checked for violations of the acceleration constraint, as discussed in the preceding section, and adjusted as necessary if the constraints are not immediately satisfied.

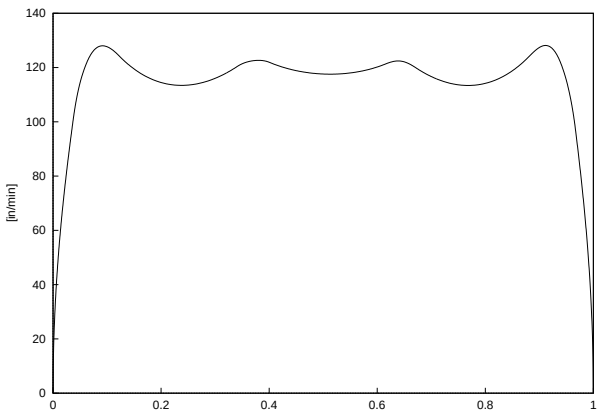

Fig. 8. Smoothed time–optimal feedrate v versus curve parameter ξ for the curve shown in Figure 6 with smoothing intervals $\Delta\xi = 0.06$.

Figure 8 shows the resulting feedrate after all the derivative discontinuities have been removed. Figure 9 compares the accelerations of the x and y axes corresponding to the original time–optimal feedrate (Figure 7) and the smoothed feedrate (Figure 8). The acceleration discontinuities apparent in the former have clearly been eliminated in the latter, while maintaining consistency with the prescribed acceleration bounds.

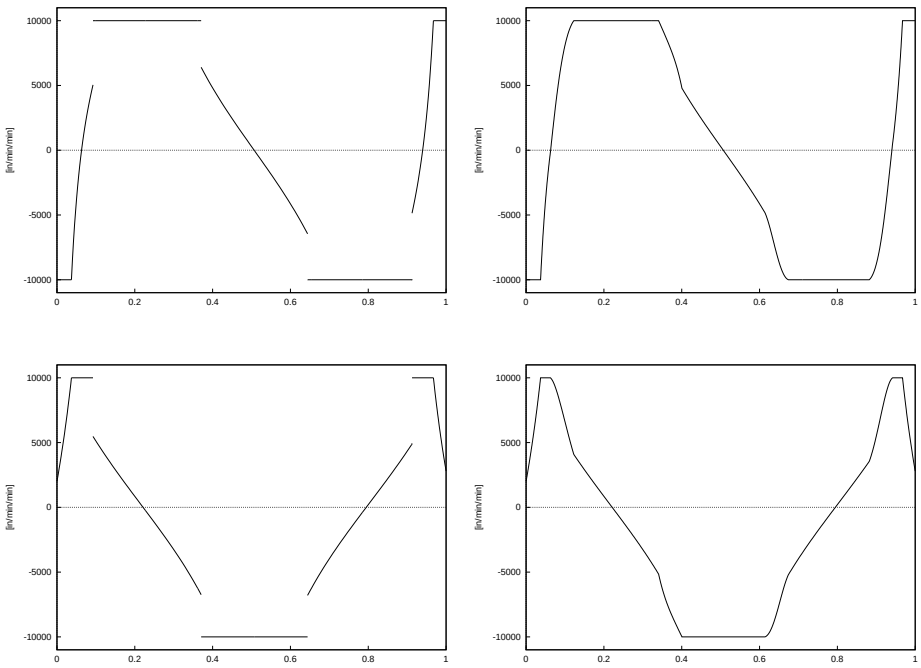

Fig. 9. Comparison of individual axis accelerations for the x (upper) and y (lower) axes versus the curve parameter ξ, corresponding to the original time–optimal feedrate shown in Figure 7 (left) and the smoothed feedrate shown in Figure 8 (right). The acceleration discontinuities incurred by the original feedrate have been eliminated with the smoothed feedrate, but the acceleration bounds $\pm 10,000$ in/min^2 are still satisfied.

4 Real–time CNC interpolator

The role of the real–time intepolator in a CNC system is to compute, at each sampling time $t_j = j\Delta t$ of the digital controller, a reference point $\mathbf{r}(\xi_j)$ along the curve in accordance with the specified feedrate variation. The actual machine position at time t_j (as measured by encoders on the machine axes) is compared with this reference point in order to generate a control signal for the axis drive motors. The elapsed time t is related to the curve parameter ξ through the interpolation integral, defined by

$$t(\xi_j) \;=\; j\Delta t \;=\; \int_0^{\xi_j} \frac{\sigma}{v}\,\mathrm{d}\xi\,. \tag{14}$$

We note that the unknown ξ_j in equation (14) is the *upper limit of integration.* In order to have an efficient and accurate real–time interpolator, capable of accommodating a variable feedrate v, it is desirable that the above integral have a simple closed–form reduction. For further background on real–time CNC interpolator algorithms, see [3, 5–7, 10, 20, 22]

If the function $t(\xi)$ has a simple closed–form expression, we can solve the equation $t(\xi_j) = j\Delta t$ by a few Newton–Raphson iterations, using the preceding reference–point parameter value ξ_{j-1} as a starting approximation. Note that $t(\xi)$, being the integral of a positive function, is monotone–increasing. Fortunately, a closed–form reduction of the interpolation integral is possible for both the unmodified time–optimal feedrate segments and the smoothing segments.

For the form (6) of the squared time–optimal feedrate (assuming that x is the acceleration–limited axis), substituting into (14) gives

$$t(\xi_j) \;=\; \int_0^{\xi_j} \frac{x'}{\sqrt{C + 2\alpha_x A_x x}}\,\mathrm{d}\xi \;=\; \frac{\sqrt{C + 2\alpha_x A_x x(\xi_j)}}{A_x} + K\,,$$

where the integration constant K is determined by the condition $\xi = 0$ at $t = 0$. Similarly, for a smoothing feedrate segment of the form (7) we obtain

$$t(\xi_j) \;=\; \int_0^{\xi_j} w\;\mathrm{d}\xi\,,$$

and since w is a polynomial, t is a polynomial of degree one higher. It is defined on the normalized interval $u \in [\,0, 1\,]$ in Bernstein form

$$t(u) \;=\; \sum_{k=0}^{6} t_k \binom{n}{k} (1-u)^{6-k} u^k.$$

by the coefficients $t_0 = 0$ and

$$t_1 = t_0 + \frac{w_0}{6}\,, \qquad t_2 = t_1 + \frac{w_1}{6}\,, \qquad t_3 = t_2 + \frac{w_2}{6}\,,$$
$$t_4 = t_3 + \frac{w_3}{6}\,, \qquad t_5 = t_4 + \frac{w_4}{6}\,, \qquad t_6 = t_5 + \frac{w_5}{6}\,.$$

5 Experimental implementation

5.1 Open–architecture CNC milling machine

The machine used in the experiments is a MillRight Compact Series 18 3–axis CNC milling machine manufactured by MHO Corporation (Figure 10), operating with the OpenCNC controller developed by Manufacturing Data Systems, Inc. Rather than the usual "black–box" type CNC controller, this system follows the open–architecture principle, allowing the user full access to all the functions and data that control the machine. In particular, custom real–time interpolators can be substituted for the standard G code interpolators. Precision ground ball–screws powered by brushless DC motors drive the three machine axes, with shaft mounted encoders providing position feedback and allowing for data collection. The digital controller operates with a sampling frequency $f = 1024\,\mathrm{Hz}$ (sampling interval $\Delta t = 1/f \approx 0.001$ sec) and a single processor provides the user interface, controls the motors, and interpolates the tool paths in real time.

Fig. 10. The MHO 3–axis mill with OpenCNC open–architecture software controller used for the time–optimal feedrate smoothing experiments.

Tool paths to be executed are transmitted to the machine in the form of *part program* files, which are read by a pre–processor that computes geometric and feedrate information prior to invoking the appropriate real–time interpolator for the type of path and feedrate to be executed. In the present context, the machine

is driven directly from the analytic description of the path as a Bézier curve, and the corresponding smoothed time–optimal feedrate functions specified in terms of piecewise–rational functions. Unlike common practice in NC part programs, it is not necessary to approximate the path by piecewise–linear/circular G codes.

5.2 Results

Figure 11 shows the measured time–optimal feedrate corresponding to an actual run of the machine along the Bézier curve shown in Figure 3 with acceleration bounds $\pm 10,000$ in/min^2 on each axis. Axis location data is measured by the encoders in each sampling interval of the digital controller, and axis velocities are computed *a posetriori* from the saved position data by first–order differencing. The feedrate is computed as the magnitude of the vector whose components are defined by the individual axis velocities. The measured feedrate profile seen in Figure 11 differs somewhat from the "theoretical" profile in Figure 4, primarily due to the fact it is plotted against the elapsed time t rather than the curve parameter ξ (these variables are related by $\mathrm{d}\xi/\mathrm{d}t = v/\sigma$).

Figures 12 and 13 show measured feedrate data from runs with the smoothed time–optimal feedrate on the same curve (Figure 3), with smoothing intervals $\Delta\xi = 0.04$ and 0.08 respectively. The traversal time for the unsmoothed feedrate was 3688 time steps Δt, whereas the smoothed feedrates required an additional 3 time steps and 7 time steps, respectively — these amount to only 0.08% and 0.19% increases in the total traversal time for the smoothed feedrates, a modest price to pay for effectively eliminating the derivative discontinuities from the time–optimal feedrate (and consequent abrupt changes in motor torque output).

Finally, Figures 14–16 show another Bézier curve and corresponding feedrates as determined from the encoder data. In this case, the unsmoothed feedrate requires 2963 time steps, and using a smoothing interval of $\Delta\xi = 0.08$ requires an additional 6 time steps (a 0.20% increase in traversal time) while eliminating the derivative discontinuities.

6 Closure

The implementation of time–optimal control on Cartesian machines with fixed acceleration bounds on each axis is particularly attractive, since this problem admits an essentially closed–form solution given a univariate polynomial root–solver to identify the feedrate break points and switching points. For a path defined by a polynomial curve $\mathbf{r}(\xi)$, the square of the time–optimal feedrate may be determined as a piecewise–rational function $q(\xi)$ of the curve parameter. Furthermore, this feedrate may be realized by a real–time CNC interpolator that works directly off the analytic curve description, obviating the need to invoke cumbersome and problematic G code [1] approximations.

The formal solution to the time–optimal feedrate problem is a C^0 function, that exhibits derivative discontinuities at certain points. Use of this function incurs instantaneous changes in the torque demand imposed on the axis drive

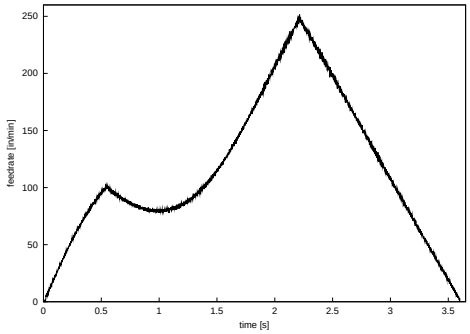

Fig. 11. Measured time–optimal feedrate for curve shown in Figure 3.

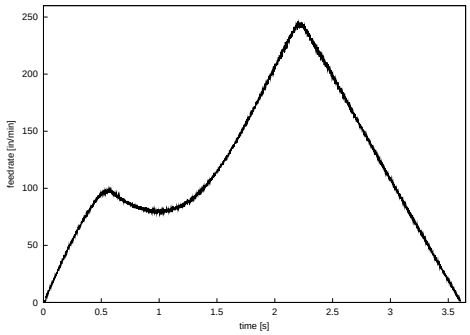

Fig. 12. Smoothed time–optimal feedrate for the curve shown in Figure 3 ($\Delta\xi = 0.04$).

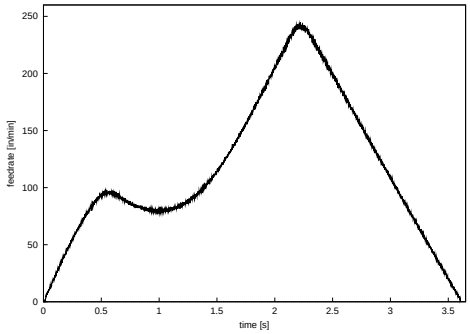

Fig. 13. Smoothed time–optimal feedrate for the curve shown in Figure 3 ($\Delta\xi = 0.08$).

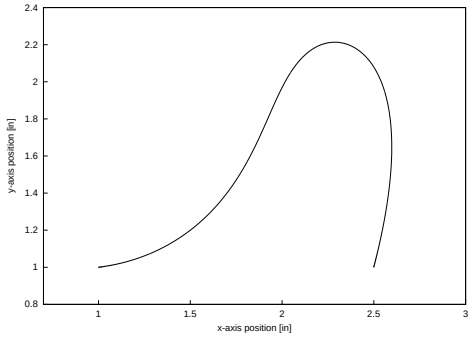

Fig. 14. Another quintic Bézier test curve for time–optimal traversal.

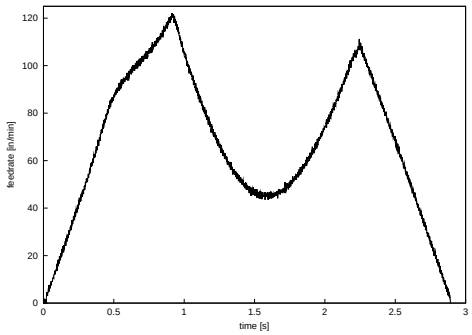

Fig. 15. Time–optimal feedrate for curve shown in Figure 14.

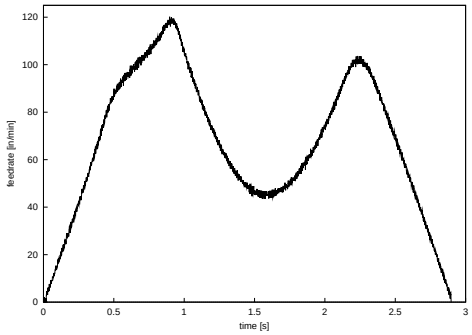

Fig. 16. Smoothed time–optimal feedrate for curve shown in Figure 14 ($\Delta\xi = 0.08$).

motors, which is physically unrealizable and may cause damage. In this paper we propose a simple scheme to remove the sudden jumps in acceleration incurred by the formal time–optimal feedrate solution. This yields a more practical, smoother motion with only a very modest (typically $< 1\%$) increase in the overall path traversal time. The smoothed feedrate coincides with the exact time–optimal feedrate over most of its extent, and the form of the smoothing elements is designed to facilitate a simple real–time CNC interpolator algorithm.

References

1. EIA Standard RS–274–D (1979), Interchangeable variable block data format for positioning, contouring, and contouring/positioning numerically controlled machines, Electronic Industries Association, Engineering Dept., Washington, D.C.
2. J. E. Bobrow, S. Dubowsky, and J. S. Gibson (1985), Time–optimal control of robotic manipulators along specified paths, *International Journal of Robotics Research* **4** (3), 3–17.
3. J.–J. Chou and D. C. H. Yang (1991), Command generation for three–axis CNC machining, *ASME Journal of Engineering for Industry* **113** (August), 305–310.
4. G. Farin (1997), *Curves and Surfaces for Computer Aided Geometric Design* (4th Edition), Academic Press, San Diego.
5. R. T. Farouki, J. Manjunathaiah, D. Nicholas, G.–F. Yuan, and S. Jee (1998), Variable feedrate CNC interpolators for constant material removal rates along Pythagorean–hodograph curves, *Computer Aided Design* **30**, 631–640.
6. R. T. Farouki and S. Shah (1996), Real–time CNC interpolators for Pythagorean–hodograph curves, *Computer Aided Geometric Design* **13**, 583–600.
7. R. T. Farouki and Y–F. Tsai (2001), Exact Taylor series coefficients for variable–feedrate CNC curve interpolators, *Computer Aided Design* **33**, 155–165.
8. C. Florian (1969), *An Introduction to the Theory of Equations*, Macmillan Company, New York.
9. H. Halkin (1965), A generalization of LaSalle's "bang–bang" principle, *SIAM Journal on Control* **2**, 199–202.
10. J.–T. Huang and D. C. H. Yang (1992), A generalized interpolator for command generation of parametric curves in computer–controlled machines, Proceedings, *Japan/USA Symposium on Flexible Automation*, Vol. 1, ASME, 393–399.
11. R. Komanduri, K. Subramanian, and B. F. von Turkovich (eds.) (1984), *High Speed Machining*, PED–Vol. 12, ASME, New York.
12. J. P. LaSalle (1960), The time optimal control problem, in *Contributions to the Theory of Nonlinear Oscillations* (L. Cesari, J. P. LaSalle, and S. Lefschetz, eds.), Vol. 5, Princeton Univ. Press.
13. F. Pfeiffer and R. Johanni (1987), A concept for manipulator trajectory planning, *IEEE Journal of Robotics and Automation* **RA–3** (2), 115–123.
14. Z. Shiller and H. H. Lu (1990), Robust computation of path constrained time optimal motions, Proceedings, *IEEE International Conference on Robotics and Automation*, Cincinnati, OH, 144–149.
15. J. J. E. Slotine and H. S. Yang (1989), Improving the efficiency of time–optimal path–following algorithms, *IEEE Transaction on Robotics and Automation* **5** (1), 118–124.
16. S. Smith and J. Tlusty (1997), Current trends in high–speed machining, *ASME Journal of Manufacturing Science and Engineering* **119**, 664–666.

17. S. D. Timar, R. T. Farouki, and C. L. Boyadjieff (2005), Time-optimal feedrates along curved paths for Cartesian CNC machines with prescribed bounds on axis velocities and accelerations, preprint.
18. S. D. Timar, R. T. Farouki, T. S. Smith, and C. L. Boyadjieff (2005), Algorithms for time-optimal control of CNC machines along curved tool paths, *Robotics and Computer-Integrated Manufacturing* **21** (1), 37–53.
19. J. Tlusty (1993), High–speed machining, *CIRP Annals* **42**, 733–738.
20. Y–F. Tsai, R. T. Farouki, and B. Feldman (2001), Performance analysis of CNC interpolators for time–dependent feedrates along PH curves, *Computer Aided Geometric Design* **18**, 245–265.
21. J. V. Uspensky (1948), *Theory of Equations*, McGraw-Hill, New York.
22. D. C. H. Yang and T. Kong (1994), Parametric interpolator versus linear interpolator for precision CNC machining, *Computer Aided Design* **26**, 225–234.